

**Ancestral Bacterial Laccase Enables Efficient Biodegradation of Inhibitory  
Wheat Straw Hydrolysate for Sustainable Microbial Protein Production**

Bo Zeng<sup>a, c, 1</sup>, Shuiping Ouyang<sup>b, 1</sup>, Zhaoxiang Wang<sup>a, c</sup>, Shixiu Cui<sup>d</sup>, Guocheng Du<sup>a, c\*</sup>,  
Song Liu<sup>a, c\*\*</sup>

<sup>a</sup> Science Center for Future Foods, Jiangnan University, Wuxi 214122, China

<sup>b</sup> College of Advanced Materials Engineering, Jiaying Nanhu University, Zhejiang  
314000, China

<sup>c</sup> School of Biotechnology, Jiangnan University, Wuxi 214122, China

<sup>d</sup> Jiaying Institute of Future Food, Jiaying, Zhejiang 314000, China

\*Corresponding author:

Address: Science Center for Future Foods, Jiangnan University, 1800 Lihu Road,  
Wuxi, 214122, China. Contact information for Guocheng Du: Phone: +86-0510-  
85918309; E-mail: [gcd@jiangnan.edu.cn](mailto:gcd@jiangnan.edu.cn)

\*\*Corresponding author:

Address: Science Center for Future Foods, Jiangnan University, 1800 Lihu Road,  
Wuxi, 214122, China. Contact information for Song Liu: Phone: +86-0510-85918307;  
E-mail: [liusong@jiangnan.edu.cn](mailto:liusong@jiangnan.edu.cn)

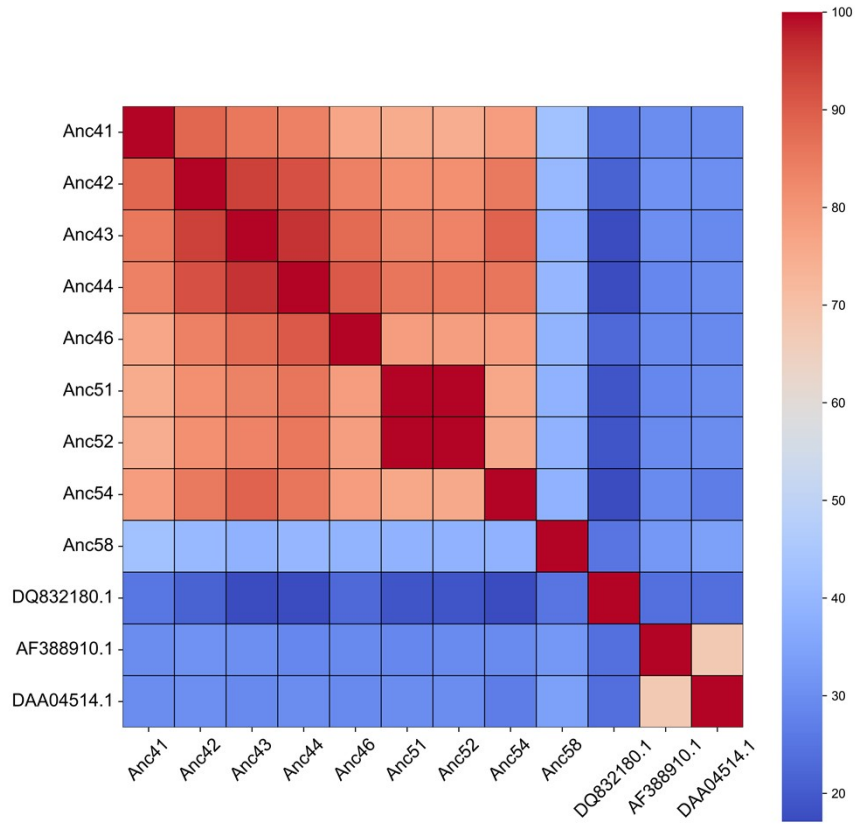


**Fig. S1.** Heatmap showing sequence similarity between ancestral laccases and previously reported laccases used for hydrolysate detoxification.

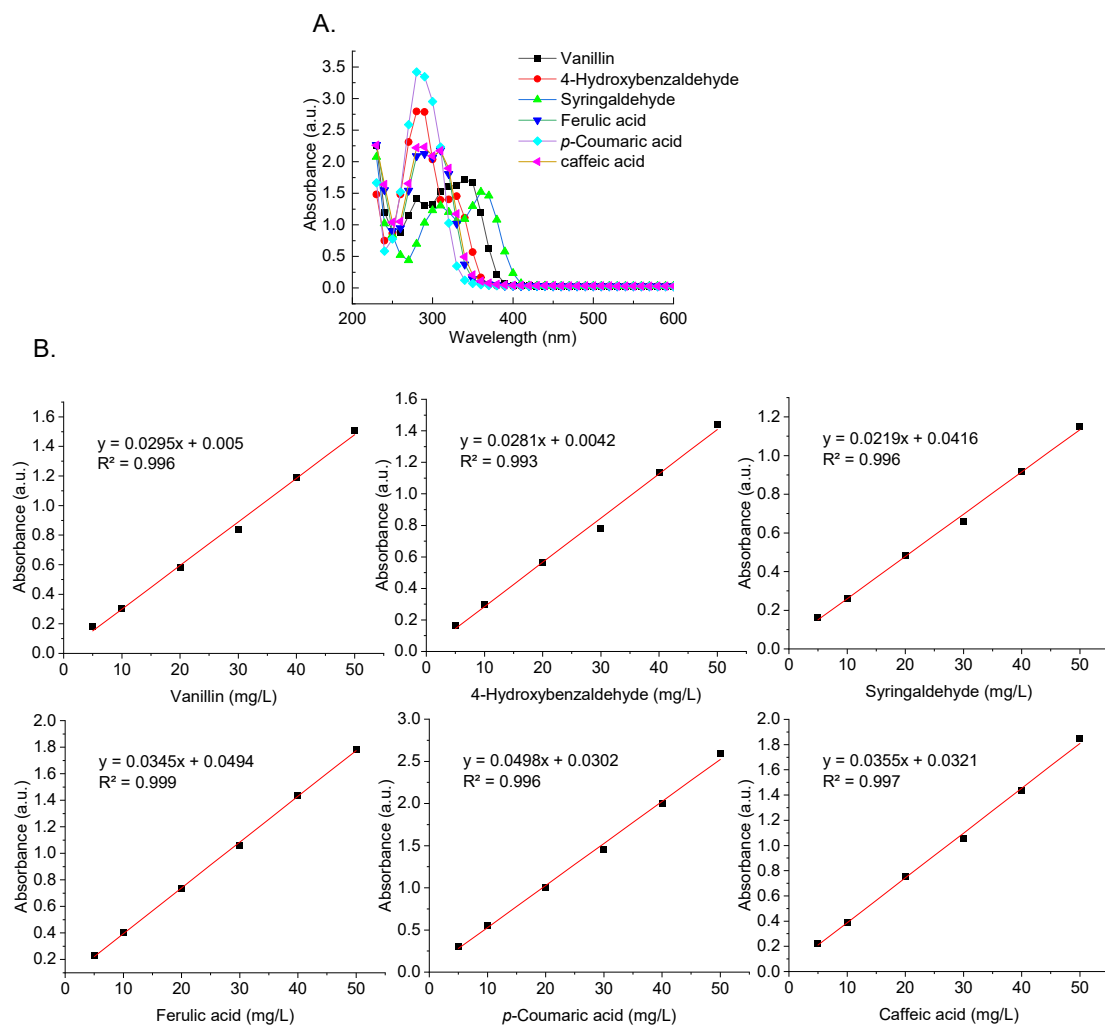


**Fig. S2.** Spectrophotometric analysis of phenolic compounds. (A). Maximum absorption wavelengths of phenolic compounds. (B) Standard curves of six phenolic compounds (5–50 mg/L).

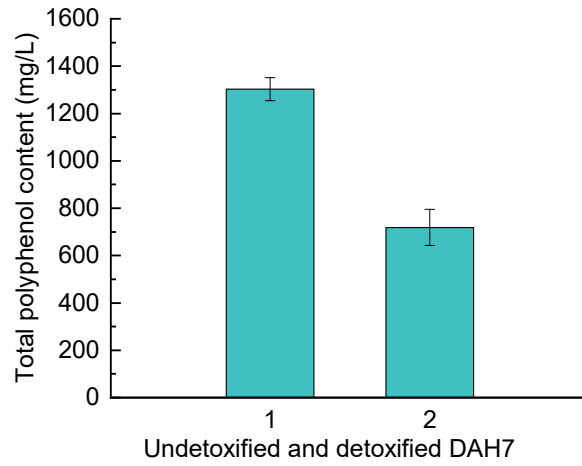


**Fig. S3.** Total phenolic content of detoxified and non-detoxified DAH7. 1. DAH7; 2. DAH7 was detoxified by Anc44. Treatment was carried out at 60°C for 24 h, with cell density  $OD_{600}$  = 30.

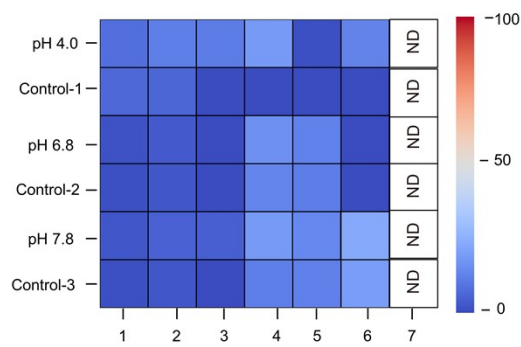


**Fig. S4.** pH-dependent degradation of seven phenolic inhibitors by *T. versicolor* laccase. Heat-map shows residual substrate (%) after 3 h reaction (at 60°C) with *T. versicolor* laccase. Substrates (50 mg/L each): 1, vanillin; 2, 4-hydroxybenzaldehyde; 3, syringaldehyde; 4, ferulic acid; 5, *p*-coumaric acid; 6, caffeic acid; 7, 4-hydroxybenzoic acid.

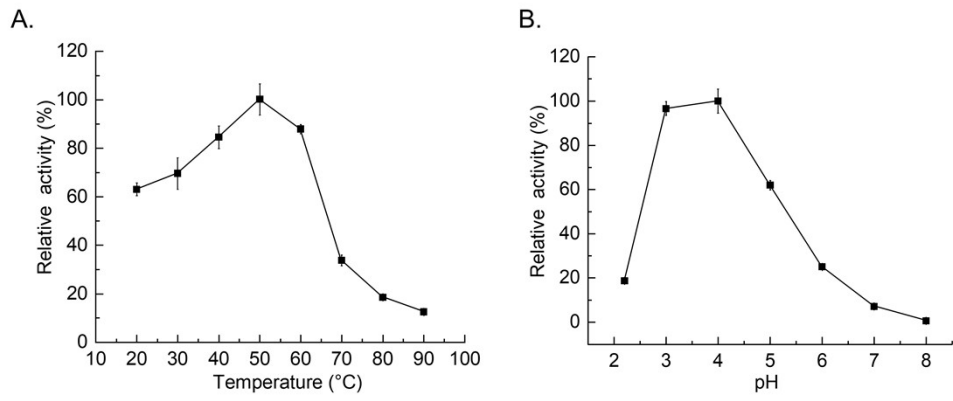


**Fig. S5.** Enzymatic characterization of the commercial laccase from *T. versicolor*. (A) Optimal temperature. (B) Optimal pH. The enzymatic activity was assayed using ABTS as the substrate.

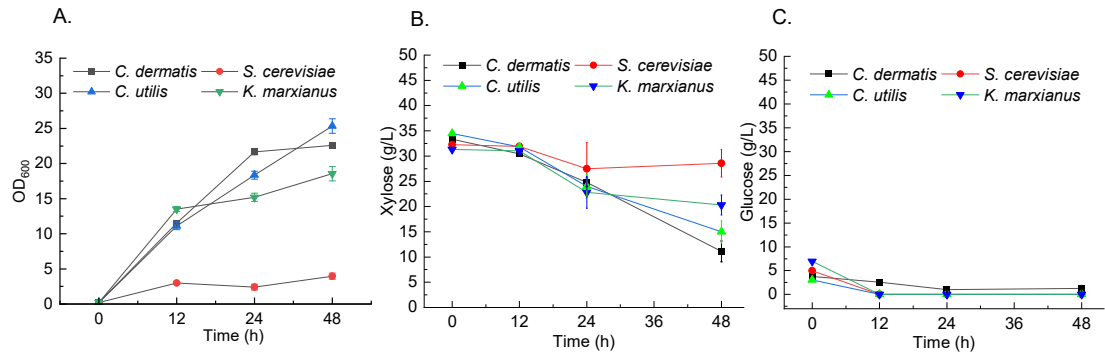


**Fig. S6.** Growth and sugar consumption profiles of yeasts in YPDX-2 media (glucose : xylose, w/w = 1:5).

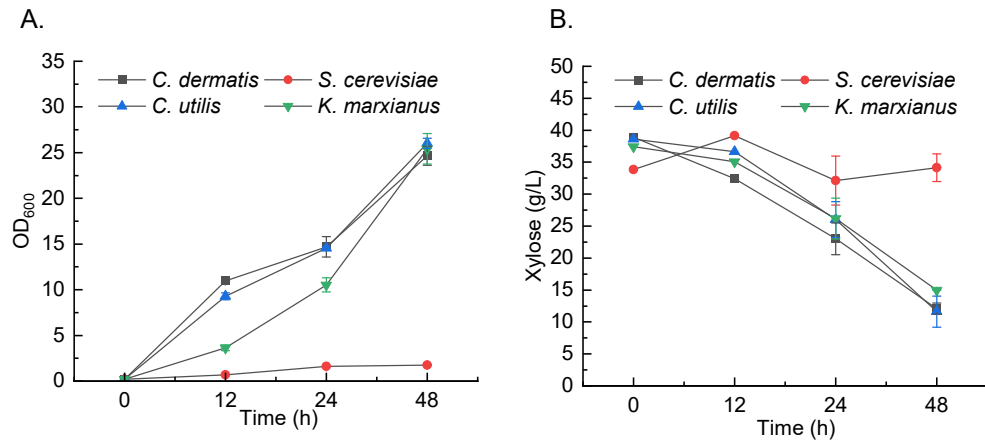
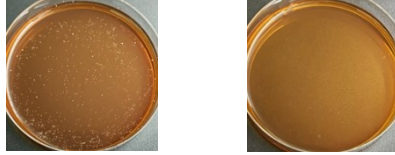


**Fig. S7.** Growth and xylose utilization profiles of yeast strains in YPDX-3 medium (xylose).



*C. utilis* ATCC 22023      *C. dermatis* ZZ-46

**Fig. S8.** Growth of *C. utilis* and *C. dermatis* on YPD<sub>X</sub>-1 plates containing 30% DAH7 treated by *E. coli* BL21 cells carrying pET-28a(+). Detoxification was carried out using the *E. coli* at a cell density of  $OD_{600} = 5$  for 24 h at 60°C.

The percentage of DAH7 treated with Anc44

---

50%

70%

100%



**Fig. S9.** Growth of *C. utilis* ATCC 22023 on YPDX-1 plates containing a high concentration of DAH7 detoxified by Anc44 at a cell density of  $OD_{600} = 30$  for 24 h at 60°C.

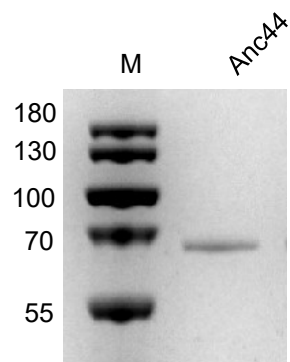


**Fig. S10.** SDS-PAGE analysis of Anc44 purified by Ni<sup>2+</sup>-affinity chromatography.

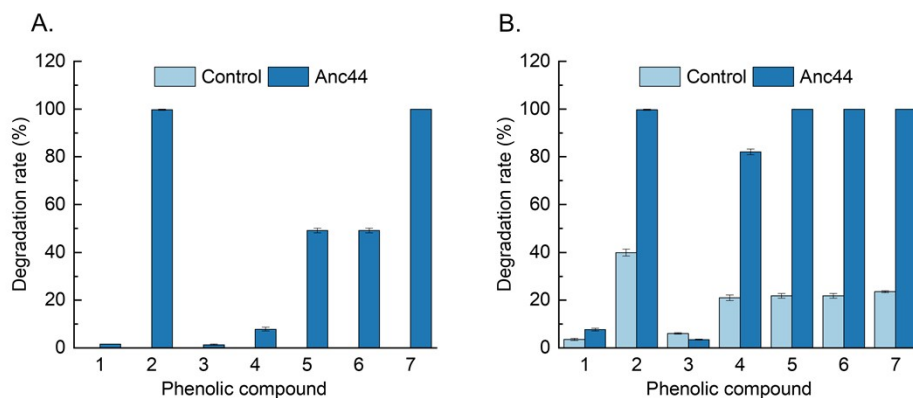


**Fig. S11.** Degradation of mixed phenolic compounds by Anc44. (A) Degradation efficiency at 0.5 h; (B) Degradation efficiency at 12 h. The phenolic compounds 1–7: 1, 4-hydroxybenzoic acid; 2, caffeic acid; 3, 4-hydroxybenzaldehyde; 4, vanillin; 5, syringaldehyde; 6, *p*-coumaric acid; 7, ferulic acid. The reaction system contained 50 mmol/L  $\text{NaH}_2\text{PO}_4\text{-C}_6\text{H}_8\text{O}_7$  buffer (pH 6.8), Anc44 (0.05 mg/L), and a mixture of seven phenolic compounds (200 mg/L each). All stated concentrations are final. Reactions were incubated at 60°C with shaking at 400 rpm for 0.5 and 12 h. Blank controls were prepared by replacing the enzyme with an equal volume of  $\text{NaH}_2\text{PO}_4\text{-C}_6\text{H}_8\text{O}_7$  buffer.

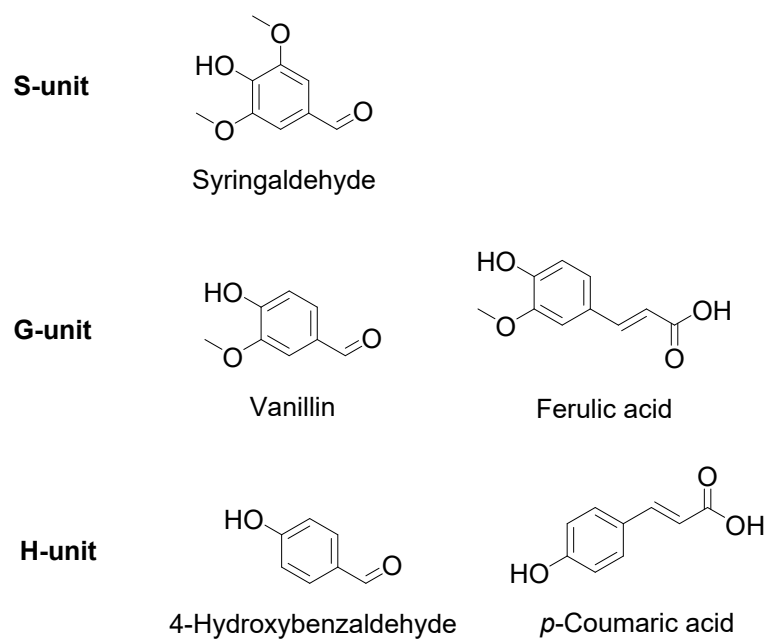


**Fig. S12.** Structures of the five phenolic compounds identified in DAH7.

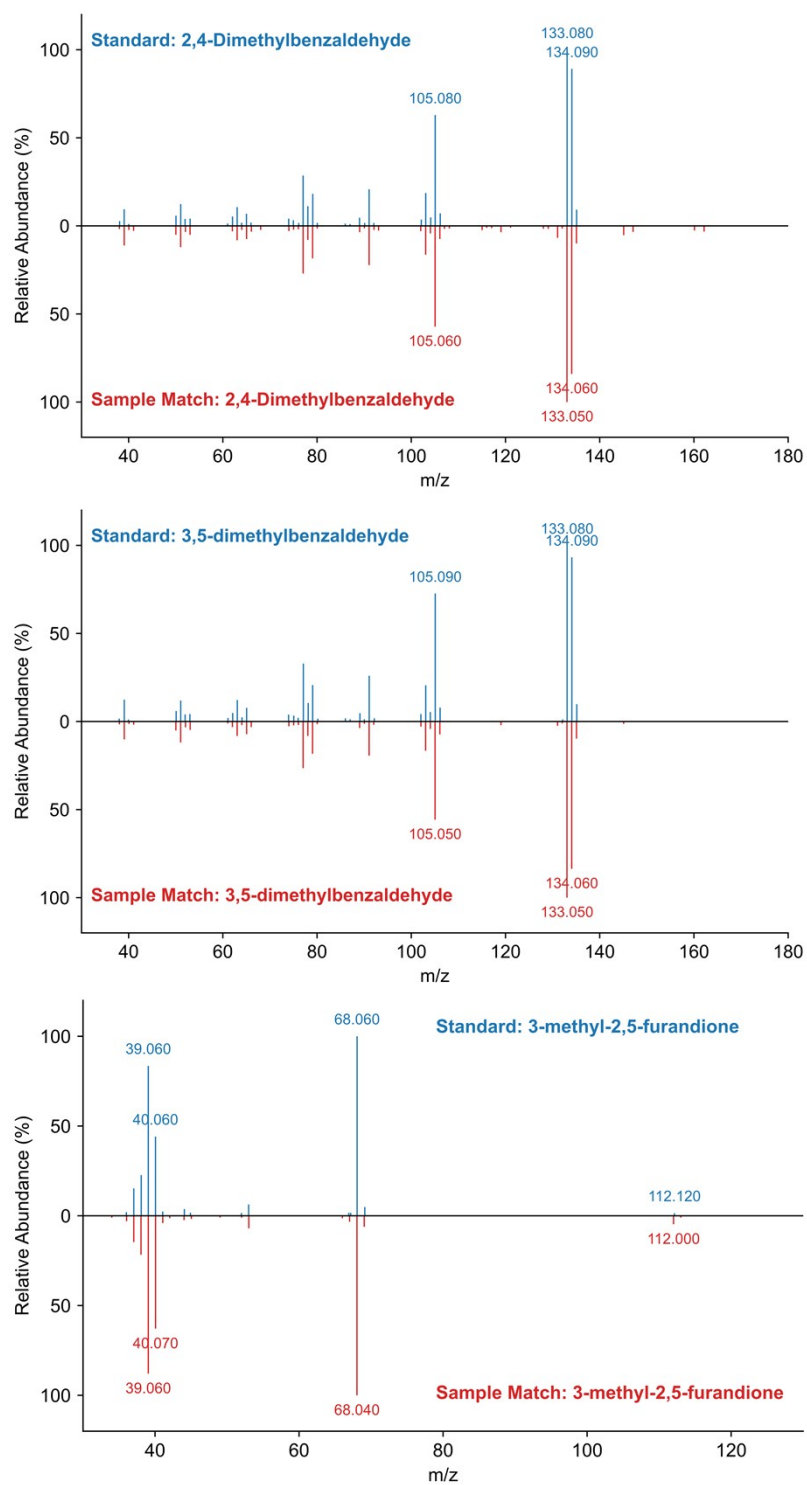


**Fig. S13.** Identification of degradation products by GC-MS with authentic standards. Head-to-tail mass spectral comparisons between detected products (bottom, red) and corresponding authentic standards (top, blue).

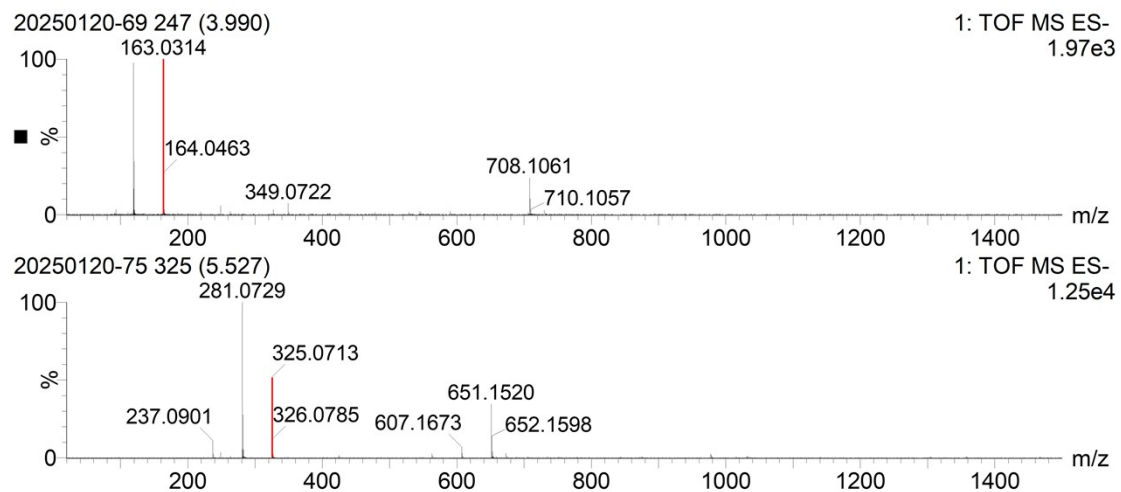


**Fig. S14.** Mass spectrometry analysis of *p*-coumaric acid degradation products catalyzed by the ancestral laccase Anc44.

**Table S1.** Mass balance and product distribution of syringaldehyde and ferulic acid degradation by Anc44.

Substrate	Product identity	Formula	Mass (mg)	Amount ( $\mu\text{mol}$ )	Molar yield (%) <sup>a</sup>
Syringaldehyde	3-methyl-2,5-furandione	C <sub>5</sub> H <sub>4</sub> O <sub>3</sub>	0.749	6.68	46.25
	3,5-dimethylbenzaldehyde	C <sub>9</sub> H <sub>10</sub> O	0.141	1.05	7.37
	Unidentified <sup>b</sup>	-	-	-	46.48
Ferulic Acid	3-methyl-2,5-furandione	C <sub>5</sub> H <sub>4</sub> O <sub>3</sub>	0.681	6.08	39.33
	2,4-dimethylbenzaldehyde	C <sub>9</sub> H <sub>10</sub> O	0.148	1.1	7.14
	Unidentified <sup>b</sup>	-	-	-	53.53

Note: Reaction conditions: Substrate (3.0 mg), 60°C, 0.5 h. Identification and quantification: Products were identified via comparison with authentic standards (MS/retention time) and quantified using external calibration curves ( $R^2 > 0.99$ ).<sup>a</sup> Molar yield calculated based on consumed substrate. <sup>b</sup> Unidentified fraction corresponds to GC-MS undetected products, presumably non-volatile or high-molecular-weight species.